ELSEVIER

Journal of Alloys and Compounds 281 (1998) 301–305

Journal of ALLOYS AND COMPOUNDS

Hydrogenation properties of $MgNi_{0.86}M1_{0.03}$ (M1=Cr, Fe, Co, Mn) alloys

Y. Tsushio[a,*], H. Enoki[b], E. Akiba[b]

[a]*Technical Research Center, Mazda Motor Corporation, 3-1 Shinchi, Fuchu-cho, Aki-gun, Hiroshima, 730-8670, Japan*
[b]*National Institute of Materials and Chemical Research, 1-1 Higashi, Tsukuba, Ibaraki, 305-8565, Japan*

Received 2 July 1998; received in revised form 27 July 1998

Abstract

Hydrogenation properties of amorphous $MgNi_{0.86}M1_{0.03}$ (M1=Cr, Fe, Co, Mn) alloys prepared by the mechanical alloying method were investigated. The Cr-substituted alloy desorbed 0.4 wt.% of hydrogen even at 423 K in the pressure range between 0.01 MPa and 1 MPa, and the enthalpy of hydride formation was calculated as -50 kJ mol^{-1} H_2^{-1}. This value is the largest among Mg-based alloys. Therefore, the hydride of this alloy is the least stable among other Mg-based alloys. However, Mn or Co-substituted alloys did not desorb hydrogen at 423 K. The influence of the substitution element on the relationship between the site energy of hydrogen in amorphous alloys and the hydrogenation properties is explained. For practical use, the Cr-substituted alloy has good enough thermodynamic properties for hydrogen storage on hydrogen vehicles though the amount of desorbed hydrogen is insufficient.

Keywords: Mg-based alloy; Substitution; Hydrogen desorption

1. Introduction

Many metal–hydrogen systems have been proposed as hydrogen storage materials. Among them, the Mg-based alloys are considered as potential candidates for hydrogen storage materials because of their large hydrogen capacity [1,2]. However, as Mg-based alloys desorb hydrogen at temperatures higher than 600 K, they are not applicable to practical use. Therefore, many studies on Mg-based alloys have been carried out to lower the desorption temperature.

Substitution is one of the most widely used methods to control or improve the hydrogenation properties of hydrogen absorbing alloys [3]. Tsushio et al. have reported on the effectiveness of substitutions on the hydrogenation properties for Mg_2Ni related alloys [4]. Tsushio et al. also modified the Mg-based Laves phase alloys, $MgNi_2$ and $MgCu_2$, by substitution [5,6]. However, they found that substitutions in Mg-based Laves phases were not effective in changing their properties because the size of the hydrogen site was too small even if the alloys were fully substituted.

Recently, hydriding properties of Mg–Ni alloys which were synthesized mechanically by ball milling have been investigated. Orimo et al. investigated the hydrogenation properties of Mg_2Ni prepared by ball milling under a hydrogen atmosphere [7]. In this system, the nanostructured composite material, which was composed of nanocrystalline and disordered Mg_2Ni, absorbed hydrogen up to 1.6wt.% and desorbed hydrogen below 440 K. Huot et al. described the effect of the presence of Mg_2Ni in the 2 Mg+Ni mixture prepared by ball milling on the onset temperature of the MgH_2 decomposition [8]. Orimo et al. reported on a new phase which was prepared from a 1:1 mixture of Mg_2Ni and Ni by ball milling [9]. The MgNi phase was amorphous and the hydriding temperature of the amorphous MgNi alloy was lowered to 373 K [9]. MgNi has a hydrogen equilibrium pressure of 3×10^{-4} MPa at room temperature [10]. The dehydriding reaction of this alloy proceeded around 0.1 MPa at 443 K [9]. However, the hydrides of those Mg–Ni based alloys prepared by the ball milling method were stable and, therefore, there is still room for improvement. Substitution of a third element into binary alloys is one of the most common techniques to control the stability of hydrides. For ball-milled alloys, few attempts have been made to modify hydrogen absorbing properties by substitution.

Therefore, in this work, we investigate the effect of substitutions on the hydrogenation properties of amorphous Mg–Ni alloys prepared by ball milling.

The amorphous MgNi absorbed hydrogen up to 2 wt.% ($MgNiH_{\sim2}$) [9]. Considering the application of hydrogen

*Corresponding author. Fax: +81-82-252-5342; e-mail: tsushio.y@lab.mazda.co.jp

0925-8388/98/$ – see front matter
PII: S0925-8388(98)00779-8

absorbing alloys in hydrogen vehicles, a rechargeable hydrogen storage capacity of over 3.0 wt.% is required. In the MgNi-based amorphous alloys, decreasing Ni content leads to a capacity increase if the H/M ratio is kept the same. Therefore, a Mg/Ni ratio of 1.16 was selected in this study. As substitution elements, we took Cr, Fe, Co and Mn.

2. Experimental procedures

2.1. Sample preparation

Mg_2Ni and $MgNi_{1.9}M1_{0.1}$ (M1=Cr, Fe, Co, Mn) were prepared by Chuo Denki Kogyo Co., Ltd. by induction melting in an Al_2O_3 crucible under a purified argon atmosphere. The ingots were crushed in air into particles of less than 100 mesh. Six grams of a 1:1 mixture of Mg_2Ni and $MgNi_{1.9}M1_{0.1}$ were milled under an argon atmosphere at 0.1 MPa. The milling was carried out in a Fritsch P5 at a rotation speed of 470 rpm for 86.4 ks at ambient temperature. The composition of the prepared alloy is $MgNi_{0.86}M1_{0.03}$ (M1=Cr, Fe, Mn, Co) and the amount of Fe contamination during milling was confirmed as 0.1 wt.% by chemical analysis.

2.2. Measurement of hydrogenation properties

The Pressure–Composition (P–C) isotherms were measured in a conventional constant-volume apparatus at 423, 473, 523 and 573 K. The measurements were carried out as follows. The powder sample was put into a vessel. The vessel was evacuated at room temperature for 10.8 ks by a rotary vacuum pump. After that, the vessel was heated to 423 K and evacuated for 10.8 ks. Then, hydrogen was introduced into the vessel at a pressure of 3 MPa at 423 K in order to reach complete hydrogenation. After measurements of the P–C isotherms during desorption at 423 K, the vessel was heated to 473 K and evacuated for 10.8 ks to desorb the remaining hydrogen in the alloy. Then, the P–C isotherms were measured at 473 K. This procedure was repeated for 523 K and 573 K in this order.

2.3. Sample characterization

The characterization of samples was performed by X-ray diffraction using a Rigaku diffractometer with a CuKα radiation for the alloys prepared by milling before hydrogenation and those evacuated for 10.8 ks by a rotary vacuum pump after the P–C isotherm measurement at 573 K.

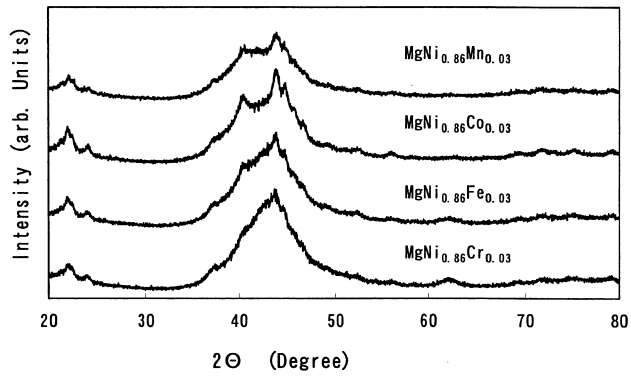

Fig. 1. X-ray diffraction profiles of $MgNi_{0.86}M1_{0.03}$ (M1=Cr, Fe, Co, Mn) after milling.

3. Results and discussion

3.1. Structure of initial compounds

Fig. 1 shows the X-ray diffraction profiles of $MgNi_{0.86}M1_{0.03}$ (M1=Cr, Fe, Co, Mn) after milling. In the case of Cr substitution, broad diffraction peaks were observed and the diffraction peaks corresponding to the intermetallic phase were not observed. In the case of Fe, Co and Mn, both the broad diffraction peak and the diffraction peaks corresponding to $MgNi_2$ were observed. However, the intensity of the peaks of $MgNi_2$ became weaker in the sequence Co, Mn and Fe. Orimo et al. reported on the structural properties of Mg–x at.% Ni (x=33, 38, 43 and 50) alloys prepared by milling for 72 ks under an argon atmosphere [9]. In the case of x=38 and 43, amorphous MgNi was partially formed. Pure amorphous MgNi was formed in the alloy Mg–50 at.% Ni. However, unreacted metallic Ni was found even in the X-ray diffraction pattern of Mg–50 at.% Ni. Orimo et al. suggested that Ni was surrounded by the amorphous MgNi. This showed that the volume fraction of amorphous MgNi increased with increasing Ni content in the range from x=33 to x=50. In this study, we selected x=45.5 and the milling time of 86.4 ks was chosen almost the same as in Ref. [9]. This is because Orimo found metallic Ni in Mg–50 at.% Ni although the amorphous phase had formed. This indicates that an almost pure amorphous phase would form for a Ni content of less than 50 at.%.

From Fig. 1 and the results of Orimo et al., we infer that an amorphous phase is present, which shows the same broad diffraction peak as the earlier reported [9] MgNi phase in $MgNi_{0.86}M1_{0.03}$ (M1=Cr, Fe, Co, Mn). The volume fraction of the amorphous MgNi phase increases in the sequence Co, Mn, Fe and Cr.

3.2. Hydrogenation properties of $MgNi_{0.86}M1_{0.03}$ (M1=Cr, Fe, Co, Mn)

Fig. 2 shows the P–C isotherms of $MgNi_{0.86}M1_{0.03}$

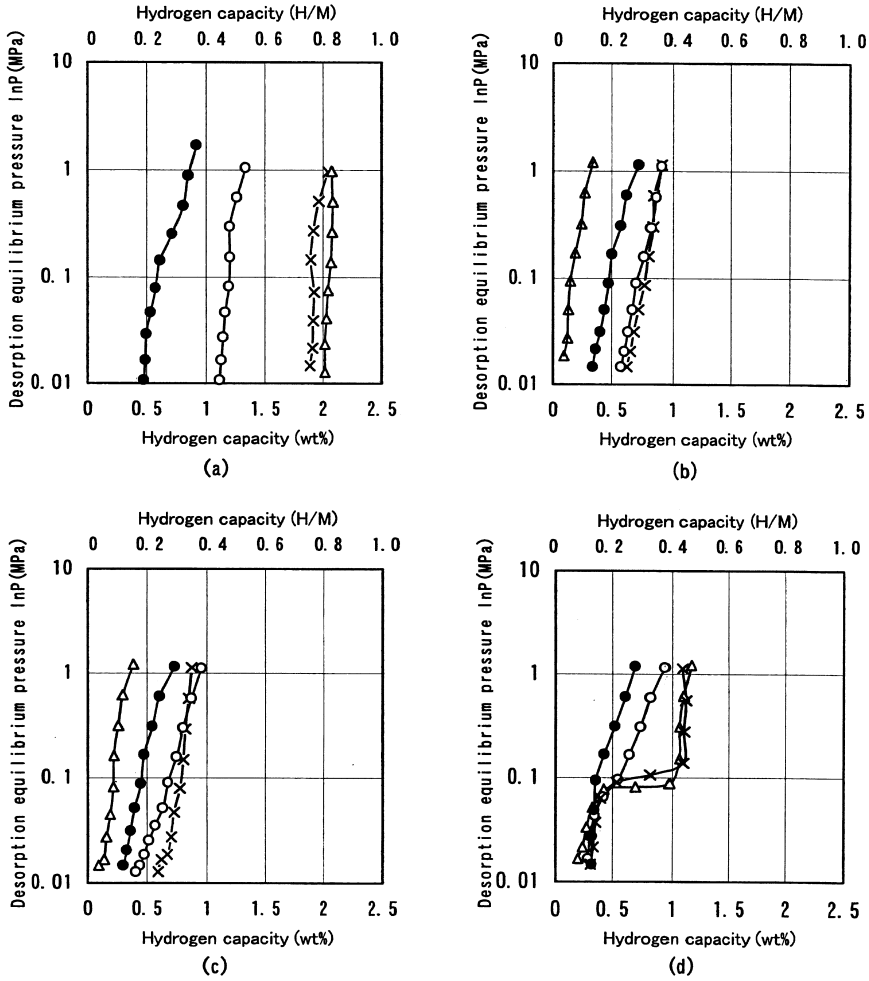

Fig. 2. Pressure–composition isotherms of the desorption for $MgNi_{0.86}M1_{0.03}$ (M1=Cr, Fe, Co, Mn). (a) 423 K (b) 473 K (c) 523 K (d) 573 K. ●: $MgNi_{0.86}Cr_{0.03}$, ○: $MgNi_{0.86}Fe_{0.03}$, △: $MgNi_{0.86}Co_{0.03}$, ×: $MgNi_{0.86}Mn_{0.03}$.

(M1=Cr, Fe, Co, Mn) at various temperatures. In the case of Cr substitution, the initial amount of absorbed hydrogen and the amount of desorbed hydrogen were 0.9 wt.% and 0.4 wt.% at 423 K, respectively. These values remained almost constant at any temperatures measured. The amount of desorbed hydrogen was defined as the width of plateau in the P–C isotherms in the pressure range between 0.01 MPa and 1 MPa. It is noteworthy that the shape of the P–C isotherm did not change even at 573 K in the case of Cr substitution. When Fe was substituted for Ni, the initial amount of absorbed hydrogen and the amount of desorbed hydrogen were 1.3 wt.% and 0.2 wt.% at 423 K, respectively. The shape of P–C isotherm is almost same as that of $MgNi_{0.86}Cr_{0.03}$ up to 523 k. The plateau of the Mg–H_2 system was observed at 573 K in $MgNi_{0.86}Fe_{0.03}$. All the P–C curves at 423 K were completely different from those of the crystalline Mg_2Ni–H_2 and Mg–H_2 systems. In the case of Co and Mn substitution, though the amount of absorbed hydrogen is 2 wt.% at 423 K, the amount of desorbed hydrogen was below 0.1 wt.% at 423 K. The plateau due to Mg–H_2 appeared above 523 K and the plateau was observed clearly at 573 K in these two alloys.

We have calculated the enthalpy of hydride formation of the Cr-substituted alloy using the van't Hoff equation. The equilibrium pressure at the center of the desorption plateau (H/M=0.3) was used for this calculation, and 130.9 $J\,mol^{-1}K^{-1}$ was used as the value of the standard entropy of hydrogen gas [11]. The enthalpy of hydride formation of the Cr-substituted alloy was found to be $-50\ kJ\,mol^{-1}$ H_2^{-1}. As mentioned before, Orimo et al. reported that amorphous MgNi showed a hydrogen equilibrium pressure of 3×10^{-4} MPa at room temperature [10]. The enthalpy of hydride formation of this alloy was $-54\ kJ\,mol^{-1}$ H_2^{-1} obtained from the same calculation. The amount of desorbed hydrogen of amorphous MgNi at 443 K was 0.05 wt.% in the pressure range between 0.1 MPa and 1 MPa [9], while that of $MgNi_{0.86}Cr_{0.03}$ at 423 K was 0.3 wt.% in the same pressure range even though the temperature was lower. We conclude that the hydride of the $MgNi_{0.86}Cr_{0.03}$ alloy is less stable than that of binary amorphous MgNi.

The amount of absorbed hydrogen of Cr, Fe, Co and Mn-substituted alloys were 0.9 wt.%, 1.3 wt.%, 2.0 wt.%, 2.0 wt.%, respectively at 423 K. Considering that the amount of absorbed hydrogen for amorphous MgNi was 2.0 wt.% [9], the increase of the ratio of Mg/Ni did not affect the amount of absorbed hydrogen.

Fig. 3 shows the X-ray diffraction patterns of $MgNi_{0.86}M1_{0.03}$ (M1=Cr, Fe, Co, Mn) evacuated for 10.8 ks after measurement of P–C isotherms at 573 K. The diffraction peaks due to the $MgNi_2$ phase and amorphous MgNi phase were observed in all alloys. The area of the broad peak due to the amorphous phase became larger in the sequence Co, Mn, Fe and Cr. Though the plateau due to the Mg–H_2 system in the P–C isotherms was observed in $MgNi_{0.86}M1_{0.03}$ (M1=Fe, Co, Mn), there was no sign of the Mg phase in the X-ray diffraction patterns. This is because the grain size of Mg is too small to be detected by diffraction. In other words, Mg exists in nanocrystalline form in $MgNi_{0.86}M1_{0.03}$ (M1=Fe, Co, Mn).

It is well known that Zr–Ni alloys form amorphous metal hydrides [12]. A plateau was not observed in the P–C isotherms of these systems. Rush et al. compared the vibrational spectra of amorphous and crystalline TiCuH [13]. In the case of the crystalline sample, the width of the frequency distribution was narrow. However, though the center of the peak existed at the same frequency in the amorphous alloy, the width of its frequency distribution became larger. The absence of a plateau and the wide frequency distribution indicate that the energy of the hydrogen sites are widely distributed. In other words, the continuously varying geometrical configurations in the amorphous alloy make the fluctuation in hydrogen site energies even much wider. Therefore, a distribution of chemical as well as geometrical configurations leads to a continuous distribution of site energies for H atoms in amorphous alloys.

The glass-forming ability of alloys using rapid solidification of melts was summarized as follows [14]. The phase diagram of alloys that are favorable as to formation of amorphous phases has a eutectic. The glass-forming ability becomes higher when the composition of the alloy becomes closer to the eutectic composition. The ability for $MgNi_{0.86}M1_{0.03}$ (M1=Cr, Fe, Co, Mn) to form an amorphous phase can be discussed using the phase diagrams of the Mg–M1 (M1=Cr, Fe, Co) systems. In the case of Co, only $MgCo_2$ is formed as intermetallic compound in the whole range of compositions [15]. In the case of Fe and Mn, no intermetallic compound is formed and there is no eutectic in the Mg–Fe [16] and Mg–Mn [17] systems. In the case of Cr, the phase diagram of Mg–Cr is not known [18]. However, the existence of CrMg, Cr_2Mg_3, $CrMg_3$ and $CrMg_4$ was reported. Considering the number of intermetallic compounds, the number of eutectics for the Mg–Cr alloys must be the largest among the alloys studied. Consequently, it can be assumed that $MgNi_{0.86}Cr_{0.03}$ may be the most favorable alloy for the formation of an amorphous phase.

From these considerations, we discuss the effect of the various substitution elements on the distribution of the hydrogen site energy. Because of the high amorphization ability of the Mg–Cr system, we assume that the distribution of hydrogen site energy of the Cr-substituted alloy is the broadest among the alloys studied. Fig. 4 shows a schematic diagram of the distribution of hydrogen site energies for the crystalline phases of Mg_2Ni and $MgNi_{0.86}M1_{0.03}$. It is assumed that the hydrogen atom presents at the higher energy site is desorbed at lower temperature than in the Mg_2Ni phase. This amount of desorbed hydrogen at lower temperature is larger in $MgNi_{0.86}Cr_{0.03}$ than in the other substituted alloys studied because of the wide distribution of hydrogen site energies. Therefore, we conclude that this is the reason for the $MgNi_{0.86}Cr_{0.03}$ alloy to desorb 0.4 wt.% of hydrogen at 423 K. In the X-ray diffraction patterns shown in Fig. 1 and Fig. 3, the intensity of the broad peak due to the amorphous phase became large in the sequence Co, Mn, Fe

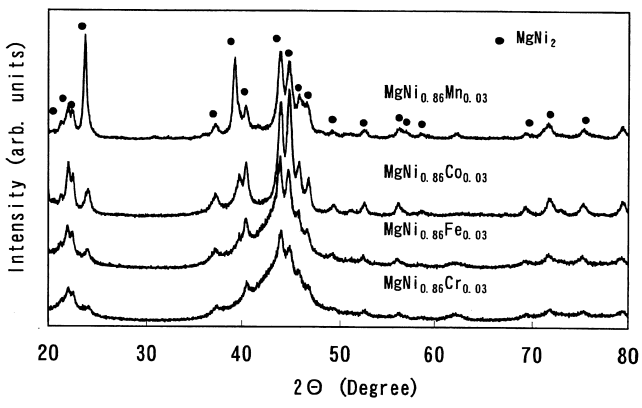

Fig. 3. X-ray diffraction patterns of $MgNi_{0.86}M1_{0.03}$ (M1=Cr, Fe, Co, Mn) evacuated for 10.8 ksec after hydrogenation at 573 K.

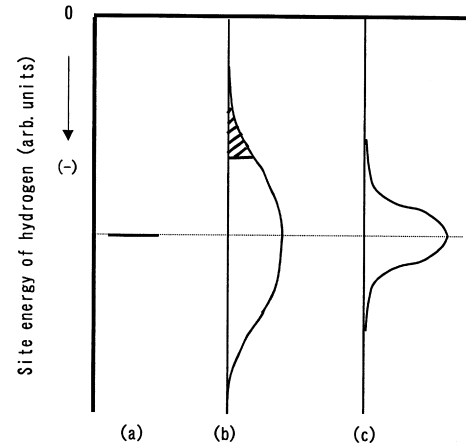

Fig. 4. Schematic diagram of the distribution of hydrogen site energies. (Shaded portion indicates the region of the hydrogen desorption at lower temperature). (a) Mg_2Ni, (b) $MgNi_{0.86}M1_{0.03}$ (M1=Cr), (c) $MgNi_{0.86}M1_{0.03}$ (M1=Fe, Co, Mn).

and Cr. This indicates that the distribution of the site energies in the Cr-substituted alloys is the widest among the alloys studied due to the high amorphization ability.

The hydrogen vehicle is the most promising and expecting application of Mg-based alloys. In view of the desorption temperature of 423 K in $MgNi_{0.86}Cr_{0.03}$, it is possible to use the engine oil as heat source for desorption of the hydrogen from this alloy. The result of this study seems to be the first step to develop new Mg-based lightweight metal hydrides for the hydrogen vehicle, though the amount of desorbed hydrogen is insufficient at this moment compared with that of $LaNi_5$.

An investigation of the effect of the Mg/Ni ratio on the hydrogen sorption properties and the thermal analysis of the alloys studied are in progress.

4. Conclusion

We investigated the effect of various substitution elements on the hydrogenation properties of $MgNi_{0.86}M1_{0.03}$ (M1=Cr, Fe, Co, Mn) in order to develop novel Mg-based alloys. The Cr-substituted alloy desorbed 0.4 wt.% of hydrogen even at 423 K in a pressure range between 0.01 MPa and 1 MPa and the hydride is the least stable among the Mg-based alloys studied. It is assumed that the desorption at low temperature is attributable to the wider energy distribution of the hydrogen sites. In other words, we are able to control the distribution of the site energies by the substitution element in the amorphous Mg–Ni based alloys.

Acknowledgements

We sincerely acknowledge to Dr. S. Orimo for valuable comments on this work.

References

[1] J.J. Reilly, R.H. Wiswall, Inorg. Chem. 7 (1968) 2254.
[2] A.S. Pedersen, B. Larsen, Int. J. Hydrogen Energy 18 (1993) 297.
[3] J.P. Darnaudery, B. Darriet, M. Pezat, Int. J. Hydrogen Energy 8 (1983) 705.
[4] Y. Tsushio, E. Akiba, J. Alloys Comp. 267 (1998) 246.
[5] Y. Tsushio, E. Akiba, J. Alloys Comp. 269 (1998) 219.
[6] Y. Tsushio, P. Tessier, H. Enoki, E. Akiba, J. Alloys Comp., in press.
[7] S. Orimo, H. Fujii, K. Ikeda, Acta. Mater. 45 (1997) 331.
[8] J. Huot, E. Akiba, T. Takada, J. Alloys Comp. 231 (1995) 815.
[9] S. Orimo, K. Ikeda, H. Fujii, Y. Fujikawa, Y. Kitano, K. Yamamoto, Acta. Mater. 45 (1997) 2271.
[10] S. Orimo, K. Ikeda, H. Fujii, S. Saruki, T. Fukunaga, A. Züttel, L. Schlapbach, Acta. Mater., in press.
[11] JANAF Thermochemical Table, 3rd ed., J. Phys. Chem. Ref. Data, 14, Suppl., 1985, p. 1.
[12] K. Aoki, M. Kamachi, T. Masumoto, J. Non-Cryst, Solids 61–62 (1984) 679.
[13] J.J. Rush, J.M. Rowe, A.J. Maeland, J. Phys. F10 (1980) L283.
[14] T.B. Massalski, Proceedings of the Fourth International Conference on Rapidly Quenched metals, Sendai Japan, 1981, p. 203.
[15] A.A. Neyeb–Hashemi, J.B. Clark, Phase Diagrams of Binary Magnesium Alloys, ASM International, 1988, p. 89.
[16] A.A. Neyeb–Hashemi, J.B. Clark, Phase Diagrams of Binary Magnesium Alloys, ASM International, 1988, p. 118.
[17] A.A. Neyeb–Hashemi, J.B. Clark, Phase Diagrams of Binary Magnesium Alloys, ASM International, 1988, p. 199.
[18] A.A. Neyeb–Hashemi, J.B. Clark, Phase Diagrams of Binary Magnesium Alloys, ASM International, 1988, p. 92.